

atom. They are given by² $(0.150 + 0.382\cos\theta + 0.324\cos^2\theta)V_2^4$ which are to be summed over neighbor pairs to each atom.

3. The Energies of the Structures

The total energy per atom contains four (electrons per atom) times the average energy of the occupied states, $-\epsilon_b$. To this we must add the overlap repulsion per atom, $\frac{n}{2}V_0(d)$. The first step is to minimize the energy for each structure with respect to the internuclear distance, d .

We do this first for the lowest-order form, Eq. (5), for ϵ_b and for the simple form $V_0(d) = A/d^4 \equiv A'V_2^2(d)$. For any compound, say GaAs, we adjust A' to obtain the minimum energy at the observed spacing in the stable structure, in this case the tetrahedral structure. We note then, however, that for that value of A' , the only dependence of the total energy upon d is through the quantity nV_2^2 appearing in Eq. (5) and in the repulsion, $nV_0(d)/2$. Thus the same value of nV_2^2 is obtained for all n , from which it follows that the equilibrium spacing varies with n as $d = Cn^{1/4}$. Further, exactly the same energy is obtained for all structures.

This might seem disappointing at first, but it in fact predicts correctly an increase in spacing with coordination (and in fact an accurate ratio of the spacings in graphite and diamond) and though the various terms in the total energy change significantly with coordination, the total energy is very nearly the same in different structures.

There are two immediate improvements to be made in our estimate. First, to replace the simplest form of V_0 by a more accurate, and steeper, form.² This favors higher coordination, an effect which is easily seen to be stronger, the larger are the metallic and polar energies in Eq. (5). This again is qualitatively correct: materials of higher metallic and higher polarity tend towards more closely packed structures. The second improvement is to add the final term from Eq. (3). That term always increases the energy and tends to grow as n^2 since it is a sum over neighbor pairs. Thus it favors low coordination and has a much stronger effect at small spacings, such as in carbon or boron nitride. The quantitative comparison with experiment, and with more accurate calculations for the energy differences between structures, and for elastic rigidity, made in Ref. 2, are not very impressive, but it may be significant that this simple and general analysis does give the correct trends from material to material. The physical origin of these trends has not been so apparent before, though careful calculations³ have in fact yielded reliable predictions of structures and of elasticity. Furthermore, the very general applicability of these forms is a feature worthy of exploring.

References:

1. W. A. Harrison, "Electronic Structure and the Properties of Solids", Freeman (New York, 1980), reprinted by Dover (New York, 1988). New parameters were introduced in W. A. Harrison, Phys. Rev. B **24**, 5835 (1981) and the A/d^4 overlap repulsion in W. A. Harrison, Phys. Rev. B **27**, 3592 (1983).
2. W. A. Harrison, Phys. Rev. B **41**, 6008 (1990).
3. See, for example, M. T. Yin and M. L. Cohen, Phys. Rev. B **26**, 5668 (1982).

LMTO AND EPM CALCULATIONS OF STRAINED VALENCE BANDS IN GaAs AND InAs

Stefan Zollner*, Uwe Schmid*, Niels E. Christensen***, Christoph H. Grein*, Manuel Cardona*, and Lothar Ley***

* Max-Planck-Institut für Festkörperforschung, Heisenbergstr. 1, D-7000 Stuttgart 80

** Institute of Physics, Aarhus University, DK-8000 Aarhus C

*** Universität Erlangen, Institut für Technische Physik, D-8250 Erlangen

We study the influence of hydrostatic pressure and (001) tensile uniaxial strain on the valence bands of GaAs and InAs along the ΓX , ΓZ , and ΓL directions for magnitudes of strain similar to those commonly found in strained-layer superlattices grown in the (001) direction.

Interest in strained semiconductors has been revived by the recent epitaxial growth of strained-layer superlattices¹ and the fabrication of strain-confined quantum well wires.² For many applications, the knowledge of the deformation potentials at high-symmetry points³ is not sufficient, but their dispersion with respect to wave vector has to be known. We have therefore calculated the dispersions of the three highest valence bands of InAs and GaAs along the ΓX , ΓZ , and ΓL directions for a typical amount of stress using the fully-relativistic linear muffin-tin orbitals (LMTO) method, based on the atom-sphere-approximation (ASA), which has been shown to give very accurate valence bands and pressure coefficients.⁴ We compare these results with bands calculated with local empirical pseudopotentials^{5,6} (EPM) and find that the EPM gives a good qualitative description of the shifts with pressure, whereas the actual magnitude of these shifts may be off by up to 50%.

As an example, we discuss the case of $\text{In}_{0.27}\text{Ga}_{0.73}\text{As}$ layers grown by MBE on GaAs substrates (i. e., lattice-mismatched) with thicknesses of 10 nm (thin) and 400 nm (exceeding the critical thickness), see Refs. 7 and 8. The lattice parameters of both layers were analyzed using x-ray diffraction. The surface of the thick layer was found to be strain-relaxed by misfit dislocations with a lattice constant of 5.762 Å, whereas the thin sample grew pseudomorphically on the GaAs substrate (5.653 Å lattice constant) and thus was tetragonally distorted in the direction of growth with a lattice constant equal to 5.837 Å. This distortion corresponds to a hydrostatic compression of 0.83% along with a tensile (001) strain contracting the lateral lattice constant by 1.07%. The results of the x-ray diffraction are similar to what is expected from elasticity theory (0.64% hydrostatic compression and 1.28% tensile strain, see Ref. 1). The valence band structures of both layers along the growth direction (ΓZ for the strained and ΓX for the unstrained case) were measured using angle-resolved photoemission^{7,8} (ARPES). Similar experiments were performed on $\text{In}_{0.2}\text{Ga}_{0.8}\text{As}$ by Hwang and co-workers,⁹ but with different results.

As band structures of alloys are difficult to calculate, we study the influence of pressure and strain on the band structure of GaAs and InAs. We refer all energies to the valence band maximum (VBM) at Γ , as neither LMTO nor ARPES can give well-defined absolute energies. We call the highest and second highest valence band heavy hole- (v_1) and light hole-like (v_2), regardless of their symmetry, and use the notation of Ref. 10. We discuss three separate cases: (i) 0.83% hydrostatic compression only, (ii) 1.07% (001) tensile strain only, and (iii) both 0.83% hydrostatic compression and 1.07% (001) tensile strain. The comparison between the strained or compressed (solid lines) and unstrained bands (dotted lines) for the three cases along the ΓZ -direction (which is equal to ΓX in the

Table 1: Strained and unstrained energies of the three highest valence bands in GaAs at high-symmetry points Γ , L , X , and Z .

GaAs	unstrained			0.83% hydrost. compression				
	Γ	X	L	Γ	X	L		
v_1	0.000	-2.821	-1.244	0.000	-2.914	-1.287		
v_2	0.000	-2.899	-1.462	0.000	-2.994	-1.509		
v_3	-0.366	-6.915	-6.667	-0.372	-6.996	-6.775		
GaAs	1.07% tensile (001) strain				strain + compression			
	Γ	Z	X	L	Γ	Z	X	L
v_1	0.000	-2.751	-2.963	-1.259	0.000	-2.824	-3.041	-1.291
v_2	-0.104	-2.831	-3.044	-1.597	-0.106	-2.899	-3.118	-1.635
v_3	-0.458	-7.146	-6.967	-6.758	-0.461	-7.322	-7.140	-6.910

hydrostatic case) as calculated with the LMTO for GaAs is shown in Fig. 1. Table I gives the calculated energies for GaAs at the high symmetry-points Γ , X , (Z), and L . Figure 2 contains the differences between the strained and unstrained bands as found from the LMTO, whereas Fig. 3 shows the same for the EPM. It is obvious that LMTO and EPM give consistent results, with the exception of the shifts of the split-off hole under uniaxial strain. Similar calculations have been performed in other symmetry directions and also for InAs, where the shifts were somewhat smaller than in GaAs (see Table II).

It can be seen that hydrostatic compression (i) shifts the two highest valence bands in GaAs at X (X_2) down by 94 meV, whereas tensile (001) strain (ii) shifts them up by 69 meV at Z (parallel to the strain) and down by 140 meV at X (perpendicular to the strain). These two effects almost cancel at Z (but not at X), when both pressure and strain are applied (iii). We also note the heavy hole-light hole splitting of 104 meV at Γ under uniaxial strain (ii), corresponding to a deformation potential $b = -1.5$ eV. The

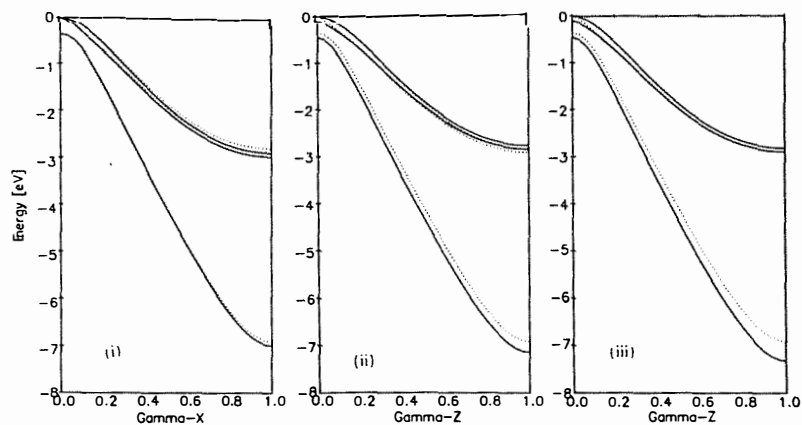


Figure 1: Band structures of strained (solid lines) and unstrained (dotted lines) GaAs for the three cases: (i) hydrostatic, (ii) tensile uniaxial and (iii) both, calculated with the LMTO method.

Table 2: Deformation potentials a for the valence bands (relative to the VBM) of GaAs and InAs at high symmetry points. At X and L , $a = \Xi_d + \frac{1}{3}\Xi_u$.

state	$\Gamma_7(v_3)$	$X_7(v_1)$	$X_6(v_2)$	$X_6(v_3)$	$L_{4,5}(v_1)$	$L_6(v_2)$	$L_6(v_3)$
GaAs	-0.24	-3.72	-3.80	-3.24	-1.86	-1.73	-4.32
InAs	-0.12	-2.92	-2.92	-3.11	-1.38	-1.25	-3.89

spin-orbit splitting Δ_0 increases by 6 meV under hydrostatic pressure (i), from which we obtain $d \ln \Delta_0 / d \ln V = p(\Delta_0) = -0.64$, in agreement with experiments on Ge and calculations for other materials.¹⁰ We note that the compressed and uncompressed split-off bands (v_3) cross twice along Δ . The split off hole shifts down by 81 meV at X_3^y under hydrostatic pressure (i), resulting in a decrease of the gap between X_3^y and X_2^y of 14 meV. The gap at Γ under uniaxial strain (ii) between v_3 and the average of v_1 and v_2 increases by 40 meV due to a quadratic effect in strain,¹⁰ the splitting between Z_3^y and Z_2^y increases by 300 meV. Under both strain and pressure (iii), this splitting changes even more (by 400 meV).

From these experiments, we expect to observe the following differences in the photoemission spectra of the strained and unstrained samples: The heavy and light hole bands (which were not resolved in photoemission) should not change their energy positions along Δ , but the shift of the split-off hole to lower energies by almost 400 meV should be observed. This is in agreement with Ref. 7, but not with Ref. 9.

We would like to thank J. D. Riley and co-workers at La Trobe University, Bundoora, Victoria, Australia, for making their data available to us prior to publication and Jordi Fraxedas for stimulating discussions and a critical reading of the manuscript.

References

¹B. Jusserand and M. Cardona, *Raman spectroscopy of vibrations in superlattices*, in

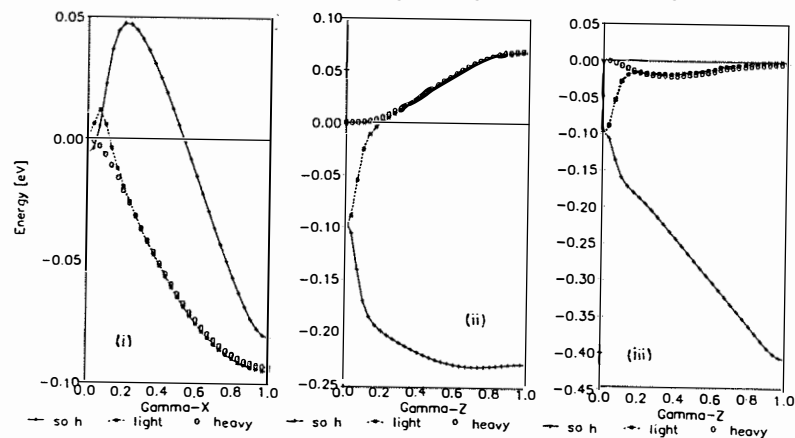


Figure 2: Differences between strained and unstrained bands in GaAs, calculated with the LMTO method.

Light Scattering in Solids V, edited by M. Cardona and G. Güntherodt, (Springer, Berlin, 1989), p. 49.

²K. Kash, B. P. Van der Gaag, J. M. Worlock, A. S. Gozdz, D. D. Mahoney, J. P. Harbison, and L. T. Florez, *Quantum confinement of excitons by strain gradients*, in *Localization and Confinement of Electrons in Semiconductors*, (Springer, Berlin, 1990), (in print).

³M. Cardona and S. Zollner, *Intra- and intervalley deformation potentials for electrons in GaAs*, in *Properties of GaAs*, EMIS Datareview Series No. 2, (INSPEC, London, 1990, 2nd edition), p. 126; S. Adachi, *Intravalley deformation potentials for holes at the Γ -point in GaAs*, *ibid.*, p. 139.

⁴N. E. Christensen, *Electronic structure of GaAs under strain*, *Phys. Rev. B* **30**, 5753 (1984).

⁵M. L. Cohen and T. K. Bergstresser, *Band structures and pseudopotential form factors for fourteen semiconductors of the diamond and zinc blende structures*, *Phys. Rev.* **141**, 789 (1966).

⁶E. Caruthers and P. J. Lin-Chung, *Pseudopotential calculations for $(\text{GaAs})_1-(\text{AlAs})_1$ and related monolayer structures*, *Phys. Rev. B* **17**, 2705 (1978).

⁷R. Leckey, J. D. Riley, and A. Stampfl, *Angle resolved photoemission using a toroidal energy analyser*, *Journal of Electron Spectroscopy and Related Phenomena* **52**, 855 (1990).

⁸A. Stampfl, G. Kemister, R. C. G. Leckey, J. D. Riley, P. J. Orders, F. U. Hillebrecht, J. Fraxedas, and L. Ley, *Band structure of InGaAs*, *J. Vac. Sci. Technol. A* **7**, 2525 (1989).

⁹J. Hwang, C. K. Shih, P. Pianetta, G. D. Kuba, R. H. Stulen, L. R. Dawson, Y.-C. Pao, and J. S. Harris, *Effect of strain on the band structure of GaAs and $\text{In}_{0.2}\text{Ga}_{0.8}\text{As}$* , *Appl. Phys. Lett.* **52**, 308 (1988).

¹⁰U. Schmid, N. E. Christensen, and M. Cardona, *Calculated deformation potentials in Si, Ge, and GeSi*, *Solid State Commun.* **75**, 39 (1990).

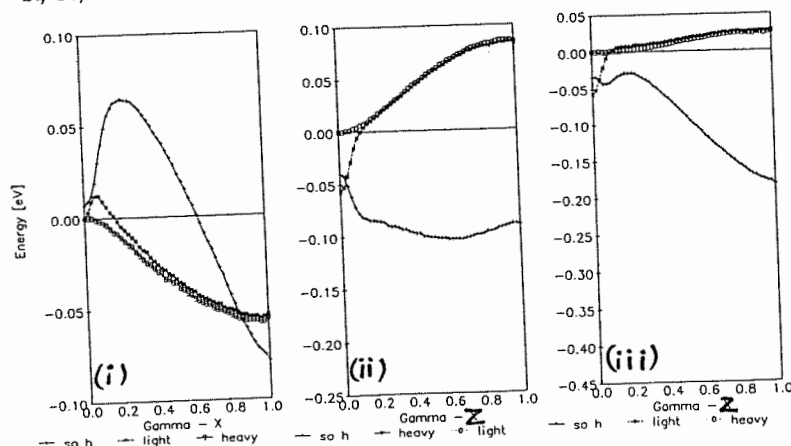


Figure 3: Differences between strained and unstrained bands in GaAs, calculated with the EPM.

First-Principles Calculation of the Vibrational Properties of $\text{Ga}_x\text{Al}_{1-x}\text{As}$ Alloys

Stefano Baroni,^a Stefano de Gironcoli,^b and Paolo Giannozzi^b

^aSISSA, Strada Costiera 11, I-34014 Trieste - Italy

^bIRRMA, PHB - Ecublens, CH-1015 Lausanne - Switzerland

The vibrational properties of $\text{Ga}_x\text{Al}_{1-x}\text{As}$ alloys have been studied from first principles using large supercells to simulate the disorder, and *ab-initio* interatomic force constants. We calculate the one-phonon Raman cross section, and discuss the mechanisms responsible for the asymmetry of the lines. In agreement with recent experiments we find that the dispersive character of phonons is not destroyed by disorder.

Despite the great technological interest of $\text{Ga}_x\text{Al}_{1-x}\text{As}$ alloys, not much is known about their vibrational properties. Due to the lack of homogeneous samples large enough for neutron diffraction studies, all the available experimental information relies on Raman spectroscopy. The one-phonon Raman spectrum of this alloy consists of two well separated main peaks (which correspond to the independent vibration of Al and Ga ions ("two-mode alloy"), and which are close to the Raman peaks of the pure materials¹), and of some very weak structures in the acoustic region, interpreted as disorder-activated longitudinal acoustic (DALA) modes. Alloying shifts and broadens the Raman peaks, also affecting their lineshape which results somewhat asymmetric.^{1b,c} This asymmetry was explained as due to disorder-activated finite- q modes:^{1b,c} as phonon bands bend downward in the pure materials, any activation of phonons with finite wavelength would result in a tail on the low-frequency side of the Raman peaks. This idea was further pursued by Parayanthal and Pollak² who suggested that the Raman line asymmetry could be explained within their "spatial correlation model", where it is assumed that: *i*) finite- q vibrations are activated by disorder in the alloy; *ii*) Raman-active modes in the alloy are localized with a correlation length $\lesssim 100\text{\AA}$. The above interpretation has been rebutted by recent Raman-scattering experiments from nonequilibrium LO phonons in $\text{Ga}_x\text{Al}_{1-x}\text{As}$, which indicate that "Raman-active LO phonons in ... $\text{Al}_x\text{Ga}_{1-x}\text{As}$ have well defined momenta and are coherent over [distances] greater than 700\AA ".³ This statement—which strictly speaking only applies to zone-center Raman-active modes—suggests that a well defined relation between frequency and wavevector for the alloy lattice vibrations could exist all over the Brillouin zone (BZ), and that the band picture of phonons is not destroyed by substitutional disorder. This picture is confirmed and extended by Raman experiments on $\text{Ga}_x\text{Al}_{1-x}\text{As}/\text{AlAs}$ superlattices (SL's):⁴ Raman peaks corresponding to phonons confined in the $\text{Ga}_x\text{Al}_{1-x}\text{As}$ region display a well defined dependence upon confinement order, thus indicating that the dispersive character of lattice vibrations persists in the bulk alloy.

All the theoretical studies performed so far on the vibrational properties of semiconductor alloys rely on phenomenological force constants, and on some kind of mean-field approximation (ATA, CPA, ...) for treating disorder. Phenomenological force constants have limited predictive power when used in the alloy, as they are usually fitted to some observed properties of one of the two crystalline constituents. This is particularly true in the case of $\text{Ga}_x\text{Al}_{1-x}\text{As}$ because very little is known about the vibrational properties of pure AlAs. Mean-field approximations, on the other hand, are not well suited for establishing the dispersive character of phonons, as the quasiparticle picture is a built-in ingredient of these approximations. The purpose of the present paper is to reexamine the mechanisms responsible for the asymmetry of the Raman lines of $\text{Ga}_x\text{Al}_{1-x}\text{As}$, and to assess the dispersive character of lattice vibrations, avoiding any unnecessary approximations. To this end, we describe the effects of disorder using large supercells (SC's) containing ≈ 500 atoms, where the cationic sites are occupied at random by Ga or Al, and obtaining the corresponding phonon frequencies and displacements by direct diagonalization of the SC

20th International Conference on

THE PHYSICS OF SEMICONDUCTORS

Volume 3

Thessaloniki, Greece
August 6 — 10, 1990

Editors

E.M. Anastassakis
N.T.U., Athens
GREECE

J.D. Joannopoulos
M.I.T., Cambridge
USA

 **World Scientific**
Singapore • New Jersey • London • Hong Kong

Published by

World Scientific Publishing Co. Pte. Ltd.

P O Box 128, Farrer Road, Singapore 9128

USA office: 687 Hartwell Street, Teaneck, NJ 07666

UK office: 73 Lynton Mead, Totteridge, London N20 8DH

Library of Congress Cataloging-in-Publication data is available.

20th International Conference on
THE PHYSICS OF SEMICONDUCTORS — Volume 3

Copyright © 1990 by World Scientific Publishing Co. Pte. Ltd.

All rights reserved. This book, or parts thereof, may not be reproduced in any form or by any means, electronic or mechanical, including photocopying, recording or any information storage and retrieval system now known or to be invented, without written permission from the Publisher.

ISBN 981-02-0539-2 (set)

ISBN 981-02-0414-0

Printed in Singapore by Loi Printing Pte. Ltd.

CONTENTS

Volume 3

VI. BULK PROPERTIES

A. Electronic and Vibrational Structure

1. Exchange and Correlation in Electronic Structure Calculations
(Invited) 1723
J. P. A. CHARLESWORTH, A. OSCHLIES, R. W. GODBY, R. J. NEEDS, & L. J. SHAM
2. Structural Stability and Interatomic Interactions in Covalent Systems 1731
W. A. HARRISON
3. LMTO and EPM Calculations of Strained Valence Bands in GaAs
and InAs 1735
S. ZOLLNER, U. SCHMID, N. E. CHRISTENSEN, C. H. GREIN, M. CARDONA, & L. LEY
4. First-Principles Calculation of the Vibrational Properties of
Ga_xAl_{1-x}As Alloys 1739
S. BARONI, S. DE GIRONCOLI, & P. GIANNOZZI
5. Relativistic Electronic Structure of the Alkali-Antimonides
and -Bismuthides: First-Principles Calculation 1743
E. V. CHULKOV, O. S. KOROLEVA, & V. M. SILKIN
6. The Heating of Electron and Spin Systems in the Narrow-Gap
Semiconductor Cd_{0.232}Hg_{0.768}Te 1747
V. I. IVANOV-OMSKII, I. A. PETROFF, V. A. SMIRNOV, J. W. TOMM, & K. H. HERMANN
7. Angle-Resolved Constant-Initial-State Spectroscopy of GaAs 1751
J. FRAXEDAS, S. ZOLLNER, L. LEY, A. STAMPFL, R. C. G. LECKEY, & J. D. RILEY
8. The Temperature Dependence of the Indirect Band Gap of Silicon:
Theory and First-Principles Calculation 1755
R. D. KING-SMITH & R. J. NEEDS
9. A Many-Body Approach to Calculating Ground-State Total Energies
of Semiconductors 1759
B. FARID, R. W. GODBY & R. J. NEEDS
10. Orbital and Spin Anisotropy of Conduction Electrons in InSb 1763
C. L. LITTLER, I. T. YOON, X. N. SONG, W. ZAWADZKI, P. PFEFFER, & D. G. SEILER